UNIVERSITY OF TWENTE.

Technical Medicine
Medical Imaging and Interventions

3D instrument tip tracking for stereotactic navigation in robot assisted Rectum resection surgery

S. Van der Heide

M2.3 report
August 2020

Supervisors:
Prof. S. Misra
Dr. C.M. Heunis
Dr. A.R. Wijsmuller

Surgical Robotics Lab
Faculty of Engineering Technology,
Department of Biomedical Engineering
University of Twente

Department of Surgery
Universitair Medisch Centrum Groningen

Contents

Chapter 1

Abstract

In 10 percent of the cases, total mesorectal excision (TME) is not radiacal in localy advance rectal carcinoma. Stereotactic surgical navigation plots the tip of the instrument on a magnetic resonance image. This image guided surgery might help the surgeon to achieve more certainty in complete tumour resection. This is often done by tracking reflective markers on the instrument and patient with two infrared cameras. Because TME is often done robot assisted, line of sight issues occur. Further, the robot wrist inside the abdominal cavity cannot be tracked with infrared markers outside the body. Two lines of tracking mechanism have been studied. The endoscopic stereo camera might be used to track the tip of the instrument. However, this method is reported as not robust and the precision is still debated. Alternately, fibre Bragg grating (FBG) shape sensors might precisely track the tip of the pose of the instrument. The main disadvantage is that this fiber must be connected to the instrument and to a marked point outside the body. This might limit the surgical function of the instrument. in our design,the FBG fiber is attached to a clamp on the tip of the surgical instrument. than it runs through a protective sleeve, through a trocard, to the infrared patient marker where it is mounted. This solution must still be tested, but when effective, it might help improve total tumour excision and might help prevent tumour recurrence

Chapter 2

Introduction

Each year, about 4500 patients are diagnosed with rectal carcinoma in the Netherlands [1]. In total 8% of those tumours grow out to be a localy advanced rectal carcinoma [2]. Depending on the tumor classification, total mesorectal excision (TME) might be needed for radical surgery in localy advanced rectal carcinoma [3], [4]. In this surgery, the rectum and mesorectum are first separated form the pelvis. Than, the rectum proximal of the tumor is dissected. Now, the distal part must be dissected. This might be done perianal, or anus sparing, depending on the tumor height and behavior [4]. This surgery is often done robotic assisted with the Da Vinci robot (Intuitive Surgical, Sunnyvale, California) In this surgery, it is important to preform a R0 resection where the whole tumor, even microscopic parts, is taken out to prevent recidivism. However, often surgery is not radical and in 10% of the cases a local recurrence occurs [5]. Magnetic resonance imaging (MRI)-images can be used to visualize the tumor, however, the perioperative position in respect to the MRI is difficult to estimate. Stereo tactic surgical navigation is a technique that is used to plot the tip of a surgical tool in real-time on preoperative computed tomography (CT)- or magnetic resonance imaging (MRI)-images. This technique is often used in rigid anatomy because the pre-and peri operative anatomy does not change [6]. However, the rectum is mostly placed retro-peritoneal which makes it less manoeuvrable witch might allow for navigation [7]. This technique can aid the surgeon's understanding of the target organ location, the route to the target anatomy, and the location to the anatomic structures close to the target organ [8]. Navigation might help to achieve more certainty in complete tumour resection [9].

In stereotactic navigation, both the instrument tip, point $t \in R^3$, and a scan $s \in R^3$ of a patient in the same operating room (OR) are visualized in the same coordinate system [8]. To do this, first, the pose of the scan must be linked with a patient marker $p \in R^3$ which is equipped with Infrared (IR) markers. A mobile c-arm, also equipped with IR markers at point $x \in R^3$, now makes a fluoroscopy image, and simultaneously a digitally reconstructed radiography (DRR) image is created. They

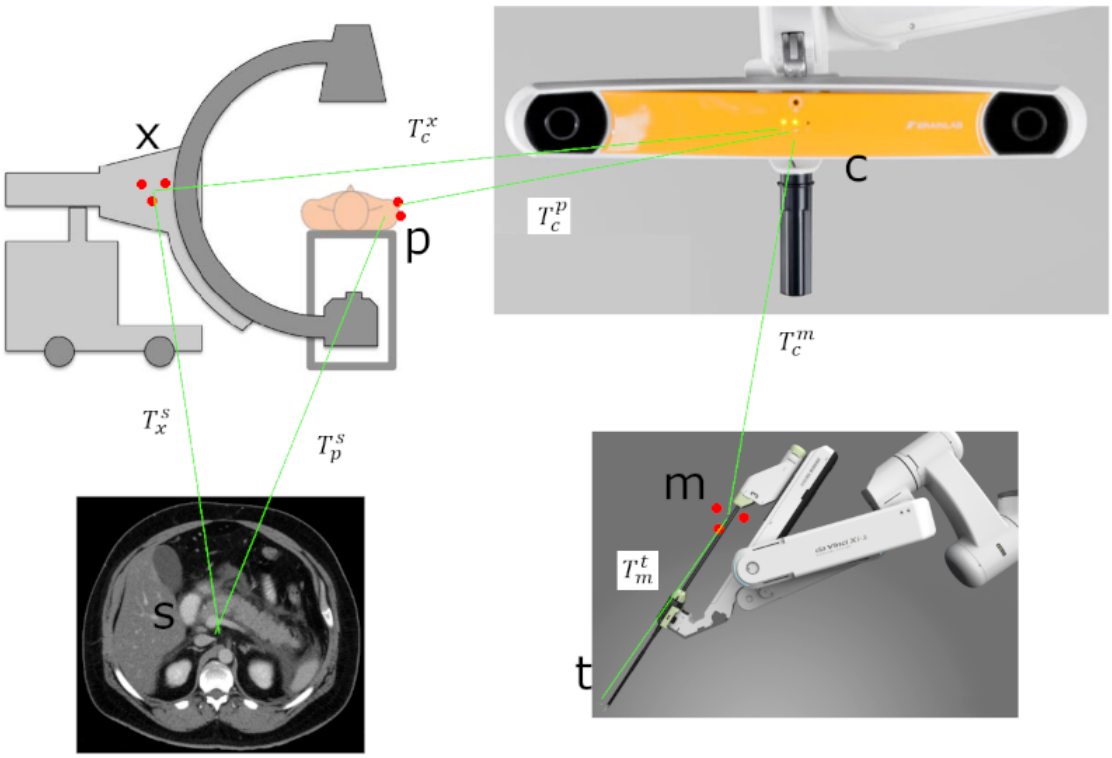

Figure 2.1: Schematic view of relevant points and transformation matrices between points for the current setup of stereotactic navigation

are compared with the use of cost function and iteratively, all translation, rotation, and scale parameters for the DRR are optimized to minimize the cost function. [10], [11] Mathematically the relation between two points i and j can be described as a transformation matrix $T_i^j = \begin{bmatrix} \mathsf{R}_i^j & p_i^j \\ 0_{1x3} & 1 \end{bmatrix} \in SE(3)$,where $R_i^j \in R^3$ is the rotation matrix and $p_i^j \in R^3$ is the transfomation vector between j en i Now, the pose of the s to point x is known in T_x^s. Because x can be tracked by the IR camera $c \in R^3$, the scan coordinates can be expressed in the coordinate system of the IR camera with T_c^x.The patient tracker pose is also expressed in OR via T_c^p. This allows to express s in p via T_p^s which discharges the need for x. In the current setup, the instrument is also equipped with IR markers at point $m \in R^3$. A transformation matrix T_m^t from t to m is obtained with a calibration. Now t can also be expressed in OR via T_c^m. Now, t and the scan are expressed in the same coordinate system which allows for navigation [11]. Figure 2.1 shows the relations of the points and transformation matrices visually [12]–[14].

Tracking surgical instruments in navigated robot surgery is suggested to be more difficult than in open or conventional laparoscopic surgery. This problem is twofold. At first, the IR markers on the surgical tool are not continuously visible to the cameras due to the line-of-sight problem. Rotations around the longitudinal axis can turn the markers behind the laparoscopic tool. Also, the extensive presence of sterile draping around the arms of the robot- and the arms itself- can occlude the line of sight. When one or both of the cameras can not see the IR markers, the system can not locate the position and pose of the instrument. This causes a loss of signal and a ‘drop-out’ of surgical navigation. To restore navigation, the cameras or robotic arms must be repositioned to achieve a line of sight. This may prolong surgical durations. The second problem is the rotation of the wrist of the instrument. The tip of the robotic instrument cannot be calibrated because the wrist can contain two hinges as seen in figure 2.2. Because of this, the exact position of the tip of the instrument relative to the IR markers. Therefore, no precise calibration is possible, which leads to inaccurate navigation. [15] Therefore, tracking tools for navigation in robotic surgery in this form is limited in drop out time and inaccuracy. A system that can accurately and robust track the tip of a robot instrument is needed.

The system needs to accomplish the following requirements.

1. The needed accuracy is estimated to be sub-centimeter for abdominal surgery to maintain patient safety. When the accuracy is lower, the navigation system may indicate a wong instrument position [16].

2. The system needs to be robust so that the surgery won’t be delayed.

Figure 2.2: The thip of a Da vinci robot tool with two hinges

3. The system should limit the function of the surgical instruments as little as possible because the surgeon must still be able to use the instrument is a surgical setting

4. The availability and possibilities of fast implementation are important because this will not limit the progress of clinical implementation.

This study compares several options for navigated laparoscopic surgery and shows the design of a setup for the most feasible option.

Chapter 3

Mechanisms for instrument tracking

3.1 Introduction

Several alternatives for IR tracking of surgical tools in laparoscopic surgery are presented in literature [16]. These alternatives include vision-based systems, shape sensors, acoustic trackers, mechanical trackers, and electromagnetic trackers. However, not all mechanisms are feasible in robotic surgery. One solution might be to use mechanical tracking of the joints of the da Vinci robot to track the position of the tip. However, the whole system is typical cable-driven, which does not allow for accurate tracking of the instrument tip, and is therefore not suitable for navigation. [16]. Electromagnetic tracking is based on measuring a current generated in small coils positioned in a magnetic field [16]. Although electromagnetic trackers have a 1.0 mm average accuracy in a good environment, accuracy will drop dramatically in robotic surgery because of sources of distortion present, such as ferromagnetic metal [17]. Acoustic trackers can determine the position of a speaker by analyzing the time of flight to three microphones. However, this method is not easily applicable from inside the abdomen or pelvis due to the differences in speed of sound, and impedance mismatch of different materials [18]. Because of this, acoustic tracking does not seem feasible in rectum surgery.

The vision and shape-based systems both seem feasible. In shape-based tracking systems, a glass fiber equipped with Fibre Bragg Grating shape sensors is placed between two points of interest. When the backscattered light though the fiber is analyzed, the strain and thus shape of the fiber can be calculated [19]. In a vision-based system, with the use of the stereo camera in the tip of the laparoscopic camera, the position of an object can be determined relative to the camera [16]. Both options are described in more detail to assess the feasibility of both options.

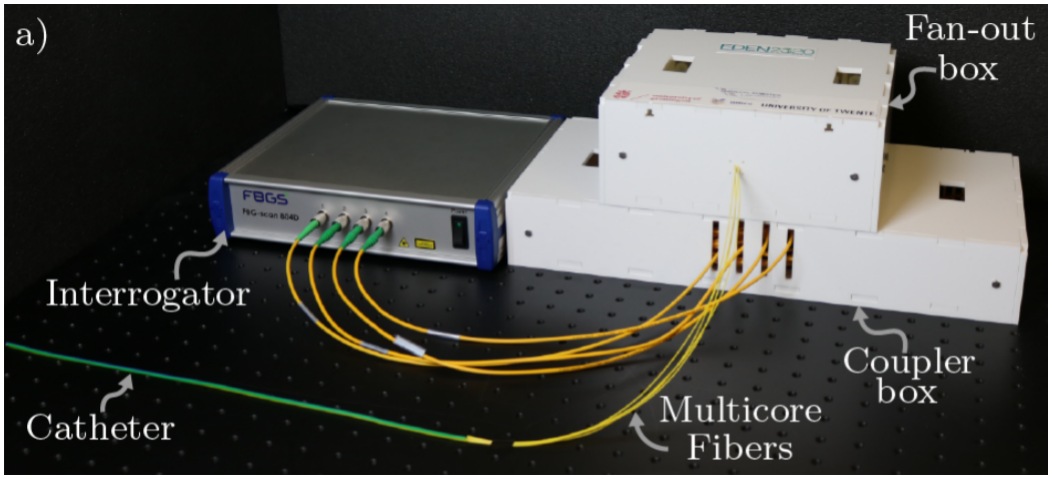

Figure 3.1: Dedicated hardware to analyze the reflected spectrum of the FBG shape sensors.

3.2 Fibre Bragg Grating shape sensors

The first proposed solution is to use multicore Fibre Bragg Grating shape sensors (FBG) to determine the position of the tip of the instrument. FBG works by sending light through the fiber. After that, the reflected spectrum is analyzed in the integrator, shown in figure 3.1 [20] the fan-out box and the coupler box separate the signals from the different cores in the fibers and merge them into the right format for the interrogator [20]. FBG fibers contain a periodically altering refractive index along the length of the fiber which backscatters the incident light in each altering. The most abundant wavelength in the reflected spectrum is called the Bragg wavelength (λ_B), given by:

$$\lambda_B = 2n_eff\Lambda \tag{3.1}$$

Where n_eff is the modal refractive index of the Bragg gratings, which is dependent on the speed of light in the gratings, and is the grating period. [19]

The backscatter from each crest of refractive index will only be in phase with the backscatter of the other crests at a wavelength two times the grating period and multiples of this. Because of the constructive interference at this wavelength and its multitudes, the power of those wavelengths in the spectrum of reflected light will be prominently present [19]. This can be seen in figure 3.2 [21]. When strain is applied on the fiber, the period of the grating's changes, which changes the reflected Bragg wavelength according to the following formula:

$$\ln \frac{\lambda_B}{\lambda_{B0}} = S(\epsilon - \epsilon_0) + \Sigma(T - T_0) \tag{3.2}$$

Where λ_{B0} is the reference Bragg wavelength, S is the gauge factor,ϵ is the strain, ϵ_0 is the reference strain, Σ is the temperature factor, T is the temperature, and T_0

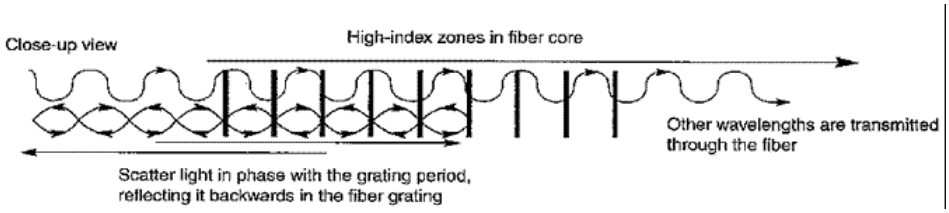

Figure 3.2: Close up view of fiber Bragg gratings. When the wavelength of light matches the wavelength of the gratings, constructive interference takes place and this wavelength, the Bragg wavelength is mainly reflected.

is the reference temperature. When $T = T_0$, the formula describes a relationship between the measured Bragg wavelength and the induced strain in the fibre [20].

Many units of Bragg gratings are placed along the length of the fiber with each a different n_eff and thus another Bragg wavelength. When multiple cores are present in the fiber, a 3D strain can be interpolated over the whole fiber. Since strain is a measure for curvature, the curvature of the fiber can be calculated for the length of the fiber. When the full curvature of the fiber is known, the position of the tip of the fiber relative to the base of the fiber is known. [22]

A catheter equipped with multicore FBG shape sensors might be used to track the position of the catheter tip. When the base of the fiber is equipped with IR markers, the position of the catheter tip relative to the patient IR markers can be known and therefore navigation is possible. The precision of this method is reported in a maximum reconstruction error of 1.05 mm in a 32 cm long fibre [20]. However, this error may increase when the fiber is longer or when strong bends of the fiber are introduced. [23] Multicore FBG shape sensors are a robust and precise technique to determine the fiber's tip position.

Despite the promising precision, to implement this into clinical practice some problems and considerations must be evaluated. The tip of the catheter cannot yet easily be fixated on the tip of the robotic instrument. The catheter is not allowed to move on the tip of the instrument because this will lead to a loss of precision. A mechanism is needed to attach the catheter to the foremost part of the instrument. Another drawback is the loss of function of the surgical instrument. Rotations around the longitudinal axis will twist the fiber around the instrument when this is fixated on the tip. Furthermore, in surgery, tissue is often separated by spreading the grasper. This action might be impeded when the fiber is attached. Therefore, the addition of a catheter to the tip of the surgical tool might limit the functionality of the instrument. However, when a good attachment mechanism is designed to allow good grasping

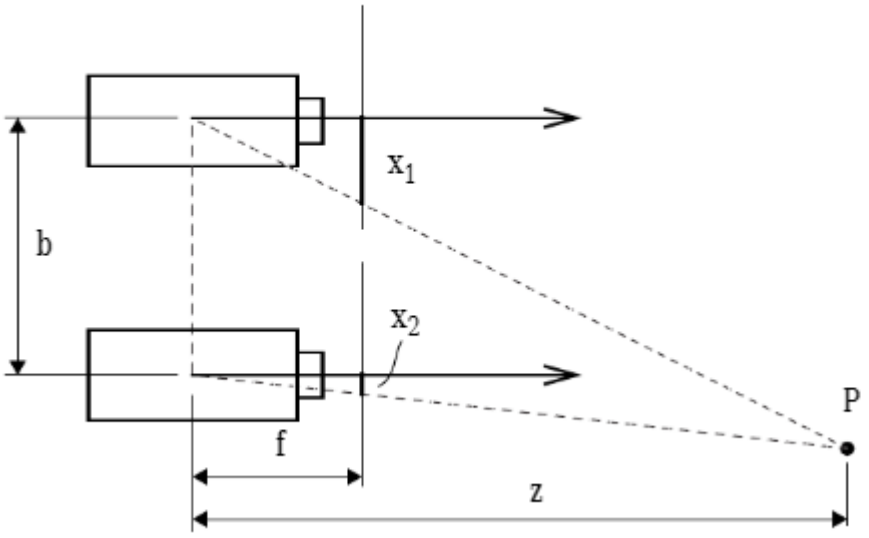

Figure 3.3: A schematic image of a stereo vision setup

and spreading function, primary functions might be preserved.

3.3 Computer vision approach

An alternative approach would be to use computer vision to estimate the position of the instrument tip. The most straight forward way to do this is to use the stereo camera from the Da Vinci system to measure disparity in the two images. The disparity is the difference between the position of a single point in two images taken from another place on the epipolar line. This is denoted as [24]:

$$d = x^1 - x^2 \tag{3.3}$$

When two camera axes are parallel, the relationship between the disparity d and depth z is:

$$d = (fb)/z \tag{3.4}$$

Where f is the focal length, and b is the length of the baseline. So when a single point is selected on both images, the depth can be calculated when b and f are known. Figure 3.3 demonstrates the camera setup [24].

The selection of the same point of the tip of the instrument in the two images is the first challenge. This selection is done based on image features. Image features are the result of any transformations of the input image. The most potent features used to detect the pose of laparoscopic instruments are color, gradient, and texture. Color, often expressed in hue, saturation, and value (HSV) is the most widespread feature

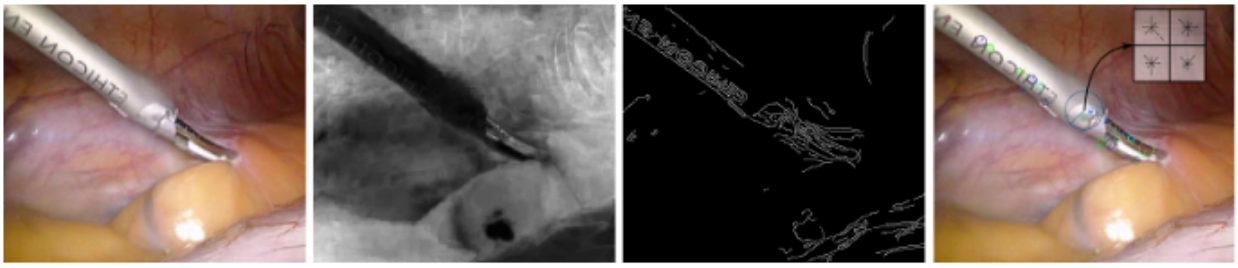

Figure 3.4: Examples of feature maps. (a) Shows a typical input image. (b) Shows a colour saturation transform. (c) Shows an edge features, and (d) shows SIFT key points

available [16]. Nearly all pose detection algorithms use this feature. However, reflections of the lighting disturb the grey metallic appearance of the instruments

The second most applied feature is the image gradient. Differentiations of an image can be done by convoluting differentiated gaussian structuring element over the input image. When an image is differentiated, a feature map for the image gradient is created. A differentiated image highlights edges. However, edges are not only found in the surgical tools, but also in the tissue surrounding the instruments which makes this feature not specific. The last important feature category is the texture, identified by keypoints. Keypoints are points of interest in the image which are automatically detected. Scale-invariant feature transform (SIFT) points are often used as successful keypoint. They are found in a scale space where two times differentiated 2D images are filtered in several grades to form a 3D scale space. SIFT points are found at extremities in this 3D scalespace, which means that they are dependent on the lines and the line frequency in the image. Figure 3.4 shows examples of the features [16].

The pose of the instrument can be found based on the found features in two ways: model/data-based, and ad hoc. Model/databases approaches compare the features in the image with the features from a model or a dataset, and thus find the position and rotation of the tool. However, these methods are advanced and often rely on machine learning and other more complex techniques. Ad hoc methods include more simple approaches to estimate the tip position such as thresholding or finding extremities. However, these methods induce bias and have little reproducibility [16].

A solution might be to introduce a color marker on the tip on the surgical in-

strument. This allows for simple ad hoc methods while being reliable and reproducable [25]. To implement this into clinical practice, a color marker for the robotic instrument should be developed.

One limitation of the usage of the stereo camera is the limited baseline length of 5.1 mm in the Da Vinci setup. The relationship between the error in depth ϵ_z and the error in disparity ϵ_d can be found by differentiating formula (2.4) towards d, which results in [26]:

$$\epsilon_z = z^2/(bf)\epsilon_d \tag{3.5}$$

The small value of b translates to a larger depth error. An average 3D error of 8.68 mm was reported as the accuracy of a Da Vinci stereo camera system [27]. However, the application of this number can be disputed since there is no zoom and thus f and depth z where considered. The application of zoom increases the focal distance f and allows for more accurate tooltip detection. Variation in distance quadratically alters the depth error concerning the disparity error. No single value for accuracy can be given for all clinical situations. To assess the theoretical accuracy, we need to estimate the focal length, the working distance, and the instrument tip localization 2D error for a given surgery.

The main advantage of this setup is the fact that nothing has to be attached to the instrument tip, which allows for free movement and full function of the instrument. The main disadvantage is its disputed accuracy and robustness [16]. Furthermore, a vision localization algorithm must be developed before implementation.

3.4 Hybrid approach

Besides stereo vision, image analysis can also be used in a combination of other techniques. In this setup, we can use FBG fibers of just IR markers to track a reference point distal on the shaft of the instrument. In this case, the position of the tip of the instrument is constrained to half a sphere around the distal joint. Image analysis might be used to find the tip of the instrument on the constrained semicircle. Visual markers can be applied to the distal shaft of the instrument to mark the reference point. Although the position of the camera and the pose of the instrument determined by IR, or FBG sensors is enough to find the semicircle on the image, additional markers on the distal end of the shaft can be used to assist to estimate the pose of the tool relative to the camera. Another hybrid approach would be to use accelerometers mounted on the instrument tip to estimate the pose of the instrument's wrist.

The advantage of this method is that no depth information has to be obtained from a stereo camera with a small base length. This might inhibit the accuracy of the system. Also, the main disadvantage of the use of FBG sensors is the fixation on the tip of the instrument. In this setup no objects, apart from markers, are attached to the tip of the instrument. The fiber can even be attached with the use of a bearing and thus allows for unlimited rotation around the longitudinal axis. Therefore, it does not limit the function of surgical instruments. Furthermore, this setup can be combined with the normal vision-based setup to increase accuracy. However, we did not find any accuracy reported by this method. The main disadvantage is that the integration of several systems leads to the stacking of errors. Al last, this setup has an increased complexity because multiple systems are combined.

3.5 Discussion

To determine which option should be used, both systems are assessed based on the pre-set requirements. The precision of FBG sensors seems is high enough for its purpose. The exact precision of the vision-based methods is yet unknown; however, some research suggests that it may be worse than the FBG‘s. Further, the FBG method is very robust, where the vision-based method may not be. Also, the FBG method is easier to implement. However, the FBG‘s main drawback is the limited function of the instrument also, the cost of FBG fibers may be higher than the vision-based method, but the no-cost evaluation has been done. When all this is taken into consideration, the FBG shape sensor method seems the best solution. A possible design will be proposed, in which the preservation of function will be considered.

Chapter 4

Design

To express point T in OR coordinates using FBG fibers, several design choices must be made. At first, the base of the fiber must be connected to any point to the instrument or another point in the operating theatre. Further, the tip of the fiber must also be attached to the tip of the instrument.

4.1 Proximal end

One of the design choices of the setup is how to relate the position of the base of the fiber to the same coordinate system as the patient tracker. The options are visualized in figure 4.1 [20], [28], [29]. The simplest solution would be to attach the base of the fiber direct to the patient maker. However, this would require a rather long fiber with many FBG sensors. The fiber must stretch from just outside the ilium, via a trocar in the abdomen, to the tip of the instrument. Because the average distance from the middle of the belly to the ilium is 15cm, the maximal length of the instrument is 33cm, and the patient marker maybe 10 cm out of the ilium, a fiber must be at least 58 cm long [30]–[32]. Because some play may be needed, the fiber with FBG sensors should be approximately 90 cm long. The part of fiber without FBG sensors must also be a few meters long to reach the hardware. Because the fibers available at the University of Twente are just 32 cm long, new fibers must be designed and fabricated. Furthermore, some sharp corners may be present, for example when the fiber enters the trocar. Both more FBG sensors and sharper corners will restrain the accuracy and more sensors are more costly [16]. For the upside though, the direct connection will remove the need for the tracking with IR markers. Since the relation of the scan to the patient marker was already known, and now also the relation between the tooltip to the patient marker, we can express the tool coordinates in the scan coordinate system.

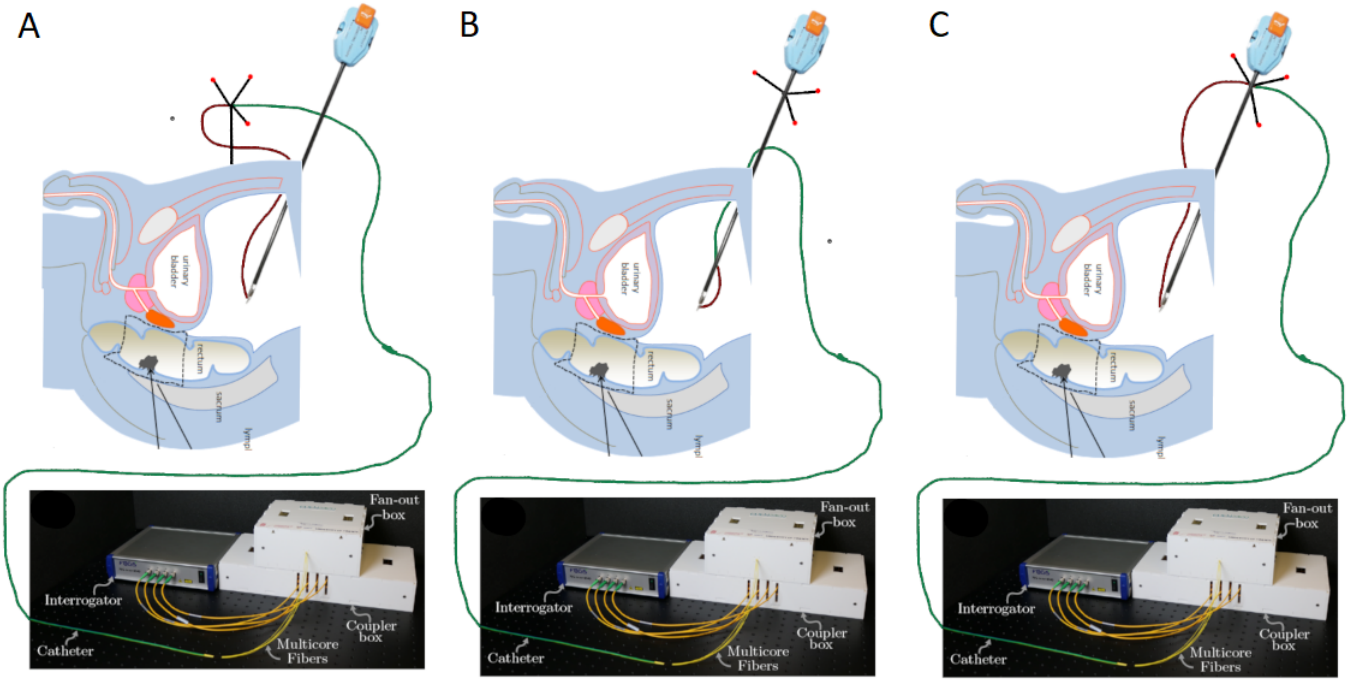

Figure 4.1: Aifferent variations to connect the base of the fiber. The brown wire represents a fiber of which the FBG sensors are used, the green wire represents a fiber without or not used FBG sensors. In a, the base is connected to a patient marker. a longer fiber is needed, but the visiblity of the infra red markers are not influenced by the instrument position. In b, the base is connected to the proximal end. the main disadvantage is the limited visibility due to line of sight problems , and in c the base is connected to the distal end of the shaft. real short fbg sensored fibers are neede. The main disadvantage is the need to attach the fiber on two poins on the instrument, and the line of sight issues as described for option B

An alternative would be to attach the base of the fiber to the proximal end of the instrument shaft. When this point is also equipped with IR markers, the position of the base can be known in OR coordinates. Because the patient marker is also equipped with markers, a vector from the patient marker to the tooltip is known. This setup would require a longer optic fiber without FBG sensors from the base to the FBG hardware. A disadvantage would be that we will still have problems with the direct line of sight of the IR markers. The line of sight was often lost because of the rotations of the IR markers. This may be solved by adding bearings to the connection with the shaft. With a bearing, the base of the fiber with IR markers can freely rotate around the shaft and thus not follow the rotations of the shaft. Now the markers do not rotate that much anymore, this problem might be addressed, however draping and the da Vinci arms might still form a problem. This problem can also be addressed with multiple IR cameras. When more cameras are used, the line of sight will be less of a problem [33].

The last variation would be to attach the base of the FBG fiber to a reference point just proximal of the tip of the instrument. An optic fiber without FBG fibers will connect the reference point to the FBG hardware. The positions of the reference point can be known by using IR markers at the proximal end of the instrument. Just a rigid calibration would lead to the position of the reference point. The main advantage would be the need for a short FBG shape sensor. A disadvantage is the need to attach the fiber on two places inside the abdomen, one on the tip, and one on the shaft. Furthermore, the line of sight of the IR markers will still form a problem, however, this might be solved with more cameras and a bearing.

In all three options, a mechanism must be developed to attach the fiber IR markers. This must be very precise because any movement will distort the position of the fiber tip. Either a calibration must take place to relate the position of the fiber base to the IR markers, or the markers must be fixated very reliable and a preprogramed calibration may be enough.

However, all options seem feasible, the solutions where the base of the fiber is attached to the instrument still need IR markers on the proximal end of the instrument. Even though there might be solutions to counter this problem, we think this is still a problem. The remaining solution is to attach the fiber to the patient marker. To do this, a longer fiber must be fabricated.

4.2 Distal end

To track the tip of the instrument, FBG fibers must be attached distally to the wrist of the instrument. This might be done via a mechanism which can fixate the fiber to the instrument, or simpler by attaching the fiber loosely via a rubber band. The

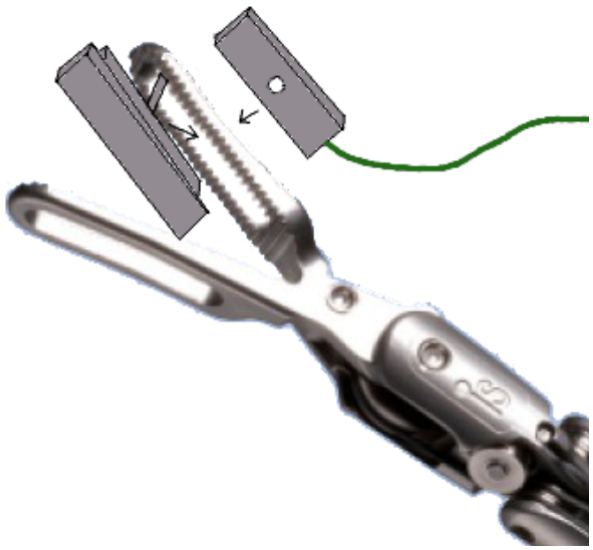

Figure 4.2: Caption

mechanism should be designed in such a way that the tip of the fiber can not move relative to the instrument. This allows for calibration of the tip of the instrument. Furthermore, the basic functions of the instrument must be preserved. Ideally, the instrument should still be able to grasp and spread tissue. An example of how this might look like is shown in figuer 4.2 [34]. A plate on with fiber can be fixated is placed on the back of the instrument. This plate is connected through the hole of a grasper to a wedge on the inside of the grasper. This setup allows the tool to remain its function. The main challenge of such a mechanism is that it must be designed and implemented.

Another challenge is the strain on the fiber. Any trocar through which the fiber enters the abdomen will have some resistance due to the air seal to maintain pneumoperitoneum. When the laparoscopic instrument is advanced in the abdomen, this resistance will pull on the fiber. In any setup, the fiber must be connected sturdy, however, the exact force of the resistance is unknown. Furthermore, since the FBG sensors are essentially strain sensors, friction might distort the position calculations of the FBG sensors. This problem might be solved by adding some overlength of the fiber in the abdominal cavity. This problem may also occur when the fiber gets twisted around the longitudinal axis. Then the strain data of the FBG sensors may be used to detect much strain in the fiber and give a warning. Furthermore, the shape data may also be used to calculate the number of twists around the longitudinal axis. If the fiber gets tangled, it can also give a warning to untwist the fiber. To conclude, a mechanism is proposed to attach the FBG fiber to the tip of the instrument. problems with strain on the fiber may be solved with several warning signs or by adding

overlength of fiber. For definitive clinical implementation, an attachment mechanism must be designed to track the tip of the instrument. Furthermore, the use of strain data of the fiber and a good attachment mechanism might solve the loss of function problems.

4.3 The fiber

khan et al proposed at the University of Twente a configuration with four sets of multicore FBG fiber with every four cores. [20] This achieves a maximum error of 1.05 mm over a length of 100mm. Since experience is present about such fibers is present at the University of Twente, this would be a good candidate for implementation. A challenge of FBG fibers is its fragile nature especially when sharp bends are introduced. To protect the fibers, they can be inscribed in a relatively stiff protective sleeve. This sleeve may protect the fiber from external impacts and may protect the fiber from sharp bending because of its stiffness. Furthermore, when the sleeve is connected to the instrument tip instead of the fiber itself, limited additional stress is applied on the fiber when the sleeve gets pulled.

The part of the fiber equiped with fbg sensors must be enveloped in the protective sleeve. The fiber should not be abel to freely rotate in the tube, because than the orrientation of the fiber tip is lost. this might be done by permanently fixating the fiber in the tube, or by creating a ridge along the length of the fiber, and an indent along the length of the tube. In this way, the fiber cannot rotate, and can maintain a orientation. At the proximal end of the sleeve, the fiber must be connected to the patientmarker in the right orientation. A marking may be used to lineup the orientation of the fiber to the orrientation of the patientmarker. the distal end may be seen in figure 4.4This may be made failsafe by designing a clamp wich can only be connected to the tube in one orrientation. The distal end of tube and fiber must be connected to a stiff attachment mechanism as seen in figure 4.3X. The fiber is connected under an angle, because a parallel connected fiber might endure more stress when the grasper is opened.

Figure 4.3: A sketch of how the tip of the instrument may be connected to the fiber. A mechanism of how this might look like is shown

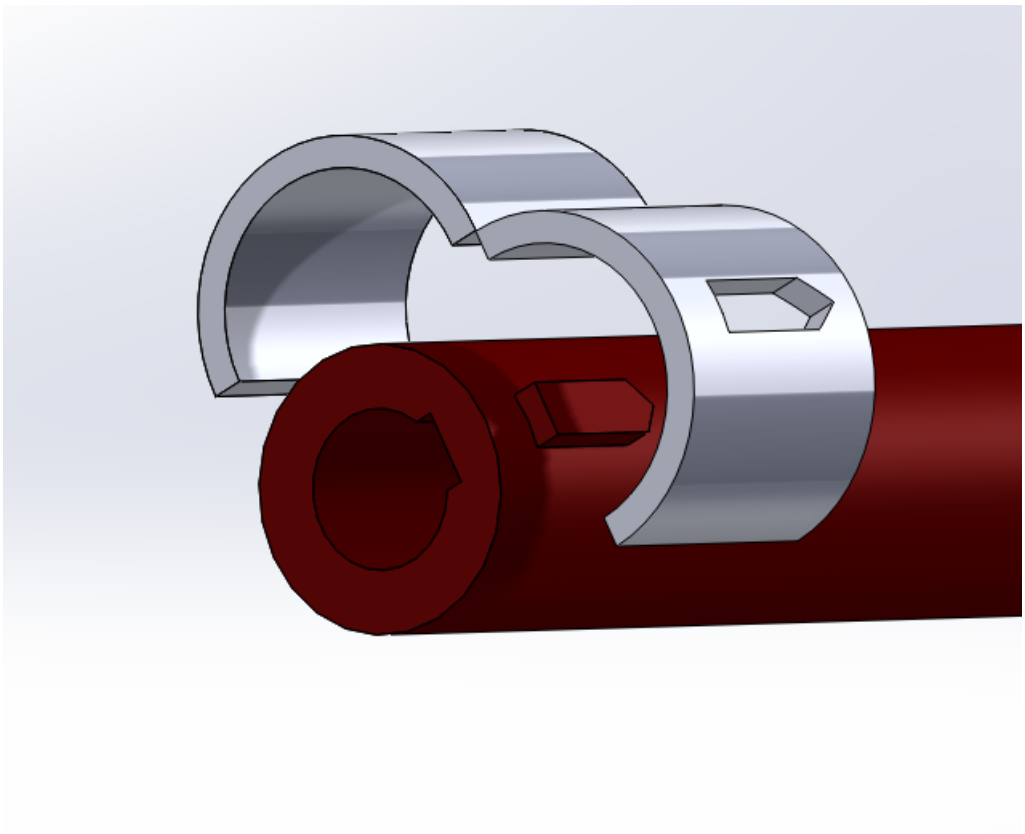

Figure 4.4: A sketch of how the base of the fiber may be connected to the an other object. A mechanism of how this might look like is shown the red tube is the sheet in which the fiber can be placed. the gray clamp must be connected to a object of choice

Chapter 5

Conclusions and recommendations

5.1 Future Prospectives

Because this proposal is established on many assumptions, the total setup must be tested and evaluated before implementing it into clinical practice. Also, several components must be developed. At first, the accuracy of the system must be tested. The accuracy of FBG fibers depends on the shape and length of the fibers, and thus the precise accuracy of this setup is unknown. Furthermore, the setup consists of several components, as IR markers and registration of the scan of the patient. Also, a calibration must be done to relate the fiber tip position to the instrument tip, and to relate the fiber base tot the patient marker. The whole setup must be tested to determine the accuracy of the system. Besides accuracy, other components also need evaluation. At first, the attachment mechanism to the grasper must further be developed and must be tested. Further, a mechanism must be developed to attach the base of the fiber to the patient marker. At last, the software must be developed to incorporate all systems.

5.2 Conclusion

We presented a setup in which the instrument tip can be tracked with FBG shape sensors to allow for navigated robot surgery. Although this is not the only option to track the tip of the instrument, FBG shape sensors are accurate, robust, and relatively easy to implement. In this setup, there are several options to implement the FBG sensor. We proposed a solution to attach the base of the fiber to the patient marker, and to insert the fiber into a sleeve towards the tip of the instrument. here the sleeve is connected to the tip of the fiber with an attachment mechanism. The main disadvantage of this solution is the possible loss of function and the need for

long FBG fibers. However, a good design and the use of additional data from the FBG sensors might solve the loss of function. Overall, this method seems to allow for accurate stereotactic navigation for robot surgery, although further testing must confirm the accuracy and feasibility of the whole system. When effective, this setup might be used in colorectal surgery to improve R0 resection planes and assist the surgeon to understand the patient-specific anatomy.

Bibliography

[1] "NKR Cijfers - IKNL." [Online]. Available: https://www.iknl.nl/nkr-cijfers?fs%7Cepidemiologie_id=6&fs%7Ctumor_id=434&fs%7Cregio_id=155&fs%7Cperiode_id=78%2C79%2C80%2C81%2C82%2C83%2C84%2C85%2C86%2C87%2C88%2C89%2C90%2C91%2C92%2C93%2C94%2C95%2C96%2C97%2C98%2C99%2C100%2C101%2C102%2C103%2C104%2C105%2C106%2C108%2C110&fs%7Cgeslacht_id=15&fs%7Cleeftijdsgroep_id=67%2C36%2C37%2C38%2C39%2C40%2C41&fs%7Cjaren_na_diagnose_id=16&fs%7Ceenheid_id=2&cs%7Ctype=line&cs%7CxAxis=periode_id&cs%7Cseries=leeftijdsgroep_id&ts%7CrowDimensions=periode_id&ts%7CcolumnDimensions=leeftijdsgroep_id&lang%7Clanguage=nl

[2] A. Jane D. Nacion, Y. Young Park, and N. Kyu Kim, "Contemporary management of locally advanced rectal cancer: Resolving issues, controversies and shifting paradigms," *Chinese Journal of Cancer Research*, vol. 30, no. 1, pp. 131–146, 2018. [Online]. Available: /pmc/articles/PMC5842228/?report=abstracthttps://www.ncbi.nlm.nih.gov/pmc/articles/PMC5842228/

[3] J. Leroy, F. Jamali, L. Forbes, M. Smith, F. Rubino, D. Mutter, and J. Marescaux, "Laparoscopic total mesorectal excision (TME) for rectal cancer surgery: Long-term outcomes," pp. 281–289, 2 2004.

[4] P. T. Phang, "Total mesorectal excision: Technical aspects," *Canadian Journal of Surgery*, vol. 47, no. 2, pp. 130–137, 4 2004. [Online]. Available: /pmc/articles/PMC3211930/?report=abstracthttps://www.ncbi.nlm.nih.gov/pmc/articles/PMC3211930/

[5] R. Berardi, "Locally advanced rectal cancer: The importance of a multidisciplinary approach," *World Journal of Gastroenterology*, vol. 20, no. 46, p. 17279, 12 2014. [Online]. Available: http://www.wjgnet.com/1007-9327/full/v20/i46/17279.htm

[6] D. A. Orringer, A. Golby, and F. Jolesz, "Neuronavigation in the surgical management of brain tumors: Current and future trends," pp. 491–500, 9

2012. [Online]. Available: /pmc/articles/PMC3563325/?report=abstracthttps://www.ncbi.nlm.nih.gov/pmc/articles/PMC3563325/

[7] J. Kenig and P. Richter, "Definition of the rectum and level of the peritoneal reflection-still a matter of debate?" pp. 183–186, 2013. [Online]. Available: /pmc/articles/PMC3796725/?report=abstracthttps://www.ncbi.nlm.nih.gov/pmc/articles/PMC3796725/

[8] U. Mezger, C. Jendrewski, and M. Bartels, "Navigation in surgery," in *Langenbeck's Archives of Surgery*, vol. 398, no. 4. Springer, 4 2013, pp. 501–514. [Online]. Available: /pmc/articles/PMC3627858/?report=abstracthttps://www.ncbi.nlm.nih.gov/pmc/articles/PMC3627858/

[9] S. Atallah, B. Martin-Perez, and S. Larach, "Image-guided real-time navigation for transanal total mesorectal excision: a pilot study," *Techniques in Coloproctology*, vol. 19, no. 11, pp. 679–684, 7 2015. [Online]. Available: https://link-springer-com.ezproxy2.utwente.nl/article/10.1007/s10151-015-1329-y

[10] C.-J. Chang, G.-L. Lin, A. Tse, H.-Y. Chu, and C.-S. Tseng, "Registration of 2D C-Arm and 3D CT Images for a C-Arm Image-Assisted Navigation System for Spinal Surgery," 2015. [Online]. Available: http://dx.doi.org/10.1155/2015/478062

[11] J. B. Stiehl, W. H. Konermann, R. G. Haaker, and A. Hebecker, "C-Arm-Based Navigation," in *Navigation and Robotics in Total Joint and Spine Surgery*. Springer Berlin Heidelberg, 2004, pp. 17–23. [Online]. Available: https://link-springer-com.ezproxy2.utwente.nl/chapter/10.1007/978-3-642-59290-4_3

[12] "Microscope Navigation - Brainlab." [Online]. Available: https://www.brainlab.com/surgery-products/overview-neurosurgery-products/microscope-navigation/

[13] "Amin Akhshi - da Vinci Xi3 - Surgical System." [Online]. Available: https://amin.artstation.com/projects/kDDDLA

[14] A. Moataz, A. Soliman, A. M. Ghanem, M. Al-Shatouri, A. Atia, and E. A. Rashed, "Three-dimensional angiography using mobile C-arm with IMU sensor attached: Initial study," in *2015 IEEE Nuclear Science Symposium and Medical Imaging Conference, NSS/MIC 2015*. Institute of Electrical and Electronics Engineers Inc., 10 2016.

[15] S. Atallah, E. Parra-Davila, A. G. Melani, L. G. Romagnolo, S. W. Larach, and J. Marescaux, "Robotic-assisted stereotactic real-time navigation: initial

clinical experience and feasibility for rectal cancer surgery," *Techniques in Coloproctology*, vol. 23, no. 1, pp. 53–63, 1 2019. [Online]. Available: https://link-springer-com.ezproxy2.utwente.nl/article/10.1007/s10151-018-1914-y

[16] D. Bouget, M. Allan, D. Stoyanov, and P. Jannin, "Vision-based and marker-less surgical tool detection and tracking: a review of the literature," pp. 633–654, 1 2017.

[17] A. M. Franz, T. Haidegger, W. Birkfellner, K. Cleary, T. M. Peters, and L. Maier-Hein, "Electromagnetic tracking in medicine -A review of technology, validation, and applications," *IEEE Transactions on Medical Imaging*, vol. 33, no. 8, pp. 1702–1725, 2014.

[18] B. C. N. E. L. B. G. M. P. D. K. A. K. N. Hasgall PA, Di Gennaro F, "IT'IS Database for thermal and electromagnetic parameters of biological tissues," 5 2018. [Online]. Available: itis.swiss/database

[19] K. O. Hill and G. Meltz, "Fiber Bragg Grating Technology Fundamentals and Overview," *JOURNAL OF LIGHTWAVE TECHNOLOGY*, vol. 15, no. 8, 1997. [Online]. Available: https://ieeexplore-ieee-org.ezproxy2.utwente.nl/stamp/stamp.jsp?tp=&arnumber=618320&tag=1

[20] F. Khan, A. Denasi, D. Barrera, J. Madrigal, S. Sales, and S. Misra, "Multi-Core Optical Fibers with Bragg Gratings as Shape Sensor for Flexible Medical Instruments," *IEEE Sensors Journal*, vol. 19, no. 14, pp. 5878–5884, 7 2019. [Online]. Available: https://ieeexplore.ieee.org/document/8667346/

[21] J. RANI MAHAPATRA and M. CHATTOPADHYAY, "SPECTRAL CHARACTERISTIC OF UNIFORM FIBER BRAGG GRATING USING COUPLE MODE THEORY ," Tech. Rep.

[22] S. Jäckle, J. Strehlow, and S. Heldmann, "Shape Sensing with Fiber Bragg Grating Sensors: A Realistic Model of Curvature Interpolation for Shape Reconstruction," in *Informatik aktuell*. Springer Berlin Heidelberg, 2019, pp. 258–263.

[23] S. Jäckle, T. Eixmann, H. Schulz-Hildebrandt, G. Hüttmann, and T. Pätz, "Fiber optical shape sensing of flexible instruments for endovascular navigation," *International Journal of Computer Assisted Radiology and Surgery*, vol. 14, no. 12, pp. 2137–2145, 12 2019. [Online]. Available: http://link.springer.com/10.1007/s11548-019-02059-0

[24] S. Bing Kang, J. Webb, L. Zitnick, and T. Kanade, “An Active Multibaseline Stereo System With Real-Time Image Acquisition,” 1994. [Online]. Available: https://www-researchgate-net.ezproxy2.utwente.nl/publication/2313285_An_Active_Multibaseline_Stereo_System_With_Real-Time_Image_Acquisition

[25] L. Bouarfa, O. Akman, A. Schneider, P. P. Jonker, and J. Dankelman, “In-vivo real-time tracking of surgical instruments in endoscopic video,” *Minimally Invasive Therapy & Allied Technologies*, vol. 21, no. 3, pp. 129–134, 5 2012. [Online]. Available: http://www.tandfonline.com/doi/full/10.3109/13645706.2011.580764

[26] D. Gallup, J.-M. Frahm, P. Mordohai, and M. Pollefeys, “Variable Baseline/Resolution Stereo,” Tech. Rep., 2008.

[27] R. Dockter, R. Sweet, and T. Kowalewski, *A Fast, Low-Cost, Computer Vision Approach for Tracking Surgical Tools*. [Online]. Available: www.bit.ly/1npTAGr.

[28] “Intuitive Surgical 420227 Ver-05 Da Vinci S PK Dissecting Forceps 8mm — For Sale — Labx Ad 4651829.” [Online]. Available: https://www.labx.com/item/intuitive-surgical-420227-ver-05-da-vinci-s-pk-dissecting/4651829

[29] “(No Title).” [Online]. Available: http://www.discoverymedicine.com/Kjetil-Soreide/files/2011/11/discovery_medicine_no_66_kjetil_soreide_figure_2.png.jhtml?id=2|attachment_8

[30] J. P. Empana, P. Ducimetiere, M. A. Charles, and X. Jouven, “Sagittal abdominal diameter and risk of sudden death in asymptomatic middle-aged men: The Paris Prospective Study I,” *Circulation*, vol. 110, no. 18, pp. 2781–2785, 11 2004. [Online]. Available: https://www.ahajournals.org/doi/10.1161/01.CIR.0000146395.64065.BA

[31] J. A. Suskewicz and B. A. Rutgers, “Estimation of living body weight based on measurements of anterior superior iliac spine breadth and stature,” Tech. Rep., 2004. [Online]. Available: https://digitalcommons.lsu.edu/gradschool_theses

[32] “Instrument & Accessory Catalog,” Tech. Rep., 2019.

[33] F. Elsamnah, W. Sediono, O. O. Khalifa, and A. A. Shafie, “Multi-stereo camera system to enhance the position accuracy of image-guided surgery markers,” in *Proceedings - 5th International Conference on Computer and Communication Engineering: Emerging Technologies via Comp-Unication Convergence, ICCCE 2014*. Institute of Electrical and Electronics Engineers Inc., 2 2015, pp. 88–91.

[34] “Intuitive Surgical, 470093, da Vinci Xi, Intuitive Surgical da Vinci Xi ProGrasp Forceps - eSutures.” [Online]. Available: https://www.esutures.com/product/1-expired/70-intuitive-surgical/37-instruments/46255176-intuitive-surgical-da-vinci-xi-8mm-prograsp-forceps-10-uses-470093/